Contribution from the Laboratoire de Physicochimie Inorganique, Unité Associée au CNRS 419, Université Pierre et Marie Curie, 75252 Paris Cedex 05, France

# Synthesis, Structure, and $^{31}P$ and $^{183}W$ NMR Spectra of $P_4W_{14}O_{58}^{12-}$

René Thouvenot,* André Tézé, Roland Contant, and Gilbert Hervé

*Received June 4, 1987*

The $P_4W_{14}O_{58}^{12-}$ anion was obtained from the reaction of sodium tungstate and sodium phosphate in acetic acid. The structure of $K_{12}P_4W_{14}O_{58}\cdot 21H_2O$ (monoclinic, $C2/c$; $a$ = 22.145 (6) Å, $b$ = 15.823 (2) Å, $c$ = 21.860 (4) Å, $\beta$ = 109.54 (2)°; $Z$ = 4) has been refined to final indices $R$ and $R_w$ of 0.048 and 0.055. The polyanion consists on two $PW_7O_{29}$ subunits linked by two phosphorus atoms. This dimeric structure is preserved in aqueous solution as shown by $^{183}W$ and $^{31}P$ NMR spectra. Unusual spin-spin coupling constants, i.e. $^2J_{W-P}$ = 18, 10.2 Hz and $^2J_{W-W}$ = 37 Hz, as well as a four-bond coupling ($^4J_{W-P}$ of about 2 Hz) are discussed in relation to the structural parameters. Some characteristic features of the vibrational (IR and Raman) spectra are also discussed.

## Introduction

The existence of several polyoxotungstophosphates[1] with a high phosphorus content (W/P < 4) was reported more than a century ago, but the first preparation of a well-defined and unequivocally characterized compound with a W/P ratio of 3.5 is due to Kehrmann.[2] Some decades later, in collaboration with Mellet,[3] he described the synthesis of $(Na_3PW_3O_{13})_n$ and of another species, probably $Na_{12}P_4W_8O_{40}$, whose crystallographic structure has been solved by Gatehouse and Jozsa.[4] By studying the solutions with weak W/P ratios, Souchay[5] denied the existence of all compounds except $PW_3O_{13}^{3-}$. A more detailed study allowed us to show that several species are in equilibrium. The solution composition depends more on its age, on the acidity, on the concentration, and on the nature of the counterion[6] than on the W/P ratio. We present here the structural characteristics in the solid state (X-ray diffraction) and in solution ($^{31}P$ and $^{183}W$ NMR) of one of the species present in the solution, namely the $P_4W_{14}O_{58}^{12-}$ polyanion.

## Experimental Section

**Syntheses. $Na_{12}P_4W_{14}O_{58}\cdot 36H_2O$.** Sodium tungstate (59 g, 180 mmol) and disodium hydrogen phosphate (10 g, 55 mmol) were dissolved in warm water (100 mL). Glacial acetic acid (40 mL, 0.7 mol) was added to the solution after cooling. The first crystals appeared after about 10 days. One week later they were filtered, washed with ethanol, and air-dried. Anal. Calcd for $Na_{12}P_4W_{14}O_{58}\cdot 36H_2O$: Na, 6.07; P, 2.72; W, 56.6; $H_2O$, 14.14. Found: Na, 6.04; P, 2.82; W, 56.2; $H_2O$, 14.3.

**$K_{12}P_4W_{14}O_{58}\cdot 21H_2O$.** Twenty-four grams of $Na_{12}P_4W_{14}O_{58}\cdot 36H_2O$ was dissolved in water (40 mL). Ten grams of potassium chloride was added. The precipitate was filtered and recrystallized in water. Anal. Calcd for $K_{12}P_4W_{14}O_{58}\cdot 21H_2O$: K, 10.49; P, 2.77; W, 57.5; $H_2O$, 8.45. Found: K, 10.45; P, 2.71; W, 57.9; $H_2O$, 8.0.

**Structure Determination.** A crystallographic study was carried out on $K_{12}P_4W_{14}O_{58}\cdot 21H_2O$. Preliminary Weissenberg photographs indicated a monoclinic lattice. The systematically absent reflections correspond to the noncentrosymmetric space group $Cc$ or the centrosymmetric space group $C2/c$. The choice of the centrosymmetric space group was consistent with the value of various statistical indicators using normalized factors and with all stages of the subsequent structure determination refinement.

The crystals are monoclinic with, at 20 °C, $a$ = 22.145 (6) Å, $b$ = 15.823 (2) Å, $c$ = 21.860 (4) Å, $\beta$ = 109.54 (2)°, $V$ = 7218.5 Å$^3$, and $Z$ = 4; $\mu$(Mo K$\alpha$) = 236.0 cm$^{-1}$.

Intensity measurements were made on a Nonius CAD 4 autodiffractometer using $2\theta_{max}$ = 50° and a graphite monochromator using Mo K$\alpha$ radiation for a specimen with dimensions of 0.36 × 0.33 × 0.27 mm glued to the end of a thin glass fiber. A total of 6358 independent reflections were collected at room temperature. A variable scan range [(1.20 + 0.345 tan $\theta$)°] and a variable scan speed (from 1.83 to 5.5°/min) were used with 25% extension at each end of the scan range for background determination. The ratio of the total background counting time to net scanning time was 1/2. The intensity data were corrected for the Lorentz and polarization factors and for absorption effect by using $\psi$ scans (the minimum and maximum correction factors were respectively 0.99 and 3.37).

The seven crystallographically independent tungsten atoms and the two phosphorus atoms were located by using direct methods (MULTAN). The potassium and oxygen atoms of the asymmetric unit were located from alternate difference Fourier syntheses and least-squares refinements. Tungsten, potassium, and phosphorus atoms were refined with anisotropic thermal parameters;[7] oxygen atoms, with isotropic ones. The final cycles of unit-weighted full-matrix least-squares refinement gave $R = \sum(||F_o| - |F_c||)/\sum F_o = 0.048$ and $R_w = (\sum w(|F_o| - |F_c|)^2/\sum wF_o^2)^{1/2} = 0.055$ for 4630 reflections having $I > 3\sigma(I)$.

All calculations were carried out with the CRYSTALS program[8] on a VAX 11725 instrument at the Laboratoire de Chimie des Métaux de Transition, Université Pierre et Marie Curie.

**NMR Spectra.** The $^{31}P$ and $^{183}W$ NMR spectra were recorded from a nearly saturated solution of the sodium salt of $P_4W_{14}O_{58}^{12-}$ in $D_2O$ (pH 5.5). The spectra were recorded in a 10-mm-o.d. tube on a WM 250 Bruker apparatus operating in the Fourier mode at 101.2 MHz for $^{31}P$ and 10.4 MHz for $^{183}W$. Chemical shifts are referenced with respect to external 85% $H_3PO_4$ contained in a capillary tube in the case of $^{31}P$ and to external 2 M sodium tungstate in 1 M NaOD in $D_2O$ in the case of $^{183}W$, in both cases in the negative convention.

Chemical shifts are given at within $^1/_{100}$ ppm for $^{31}P$ and $^1/_{10}$ ppm for $^{183}W$ although the effective reproducibility could be less due to the great sensitivity of chemical shifts to experimental conditions especially in the case of the tungsten nucleus.

## Results

**Solid-State Structure of $K_{12}P_4W_{14}O_{58}\cdot 21H_2O$.** The $P_4W_{14}O_{58}^{12-}$ anion illustrated in Figure 1 is formed of two $PW_7O_{29}$ subunits linked by two phosphorus atoms. Due to the symmetry of the cell, only half of the polyanion had to be determined. The numbering of tungsten atoms is given in Figure 1. P(1) and P(2) are respectively the central atom of the subunit and the bridging atom. Different types of oxygen atoms (Oa, Ob, Oc, Od, Od′) are distinguished in the polyanion as usual.[9] Moreover, oxygen atoms linked to P(2) are referred to as Op. Therefore, oxygen atoms are designated by their type and, in parentheses, the number of the W atoms to which they are linked.

The atomic coordinates and vibrational parameters are given with estimated standard deviations in Table I. Selected bond lengths and angles are given in Table II.

In each subunit, the tungsten atoms are arranged around the central P(1) atom in a triad of edge-sharing octahedra, a group of two edge-sharing octahedra, and two single octahedra. The junction between the $W_3O_{13}$ and the $W_2O_{10}$ groups corresponds to a part of a $\beta$ type Keggin structure. The length of the W-Oa bonds increases as the number of octahedra in the group: 2.17 Å for the single, 2.29 Å for the double, and 2.40 Å for the triad.

(1) *Gmelins Handbuch der anorganischen Chemie*; Verlag Chemie: Berlin, 1933; System No. 54 (Wolfram), p 373.
(2) Kehrmann, F. *Z. Anorg. Chem.* **1892**, *1*, 437.
(3) Kehrmann, F.; Mellet, R. *Helv. Chim. Acta* **1922**, *5*, 942.
(4) Gatehouse, B. M.; Jozsa, A. J. *Acta Crystallogr., Sect. C: Cryst. Struct. Commun.* **1983**, *C39*, 658.
(5) Souchay, P. *Ann. Chim. (Paris)* **1947**, *12*, 203.
(6) Knoth, W. H.; Harlow, R. L. *J. Am. Chem. Soc.* **1981**, *103*, 1865.
(7) The values of anisotropic thermal parameters of the K(6) atom suggest that it is perhaps disordered, but the sites are too close and we did not succeed in separating them.
(8) Carruthers, J. R.; Watkin, D. J. "CRYSTALS, an Advanced Crystallographic Program System"; Chemical Crystallography Laboratory, Oxford University: Oxford, England, 1984.
(9) (a) Robert, F.; Tézé, A. *Acta Crystallogr., Sect. B: Struct. Crystallogr. Cryst. Chem.* **1981**, *B37*, 318. (b) Canny, J.; Tézé, A.; Thouvenot, R.; Hervé, G. *Inorg. Chem.* **1986**, *25*, 2114.

0020-1669/88/1327-0524$01.50/0 

**Table I.** Fractional Atomic Coordinates and Thermal Parameters[a]

| atom | x/a | y/b | z/c | U(iso),[b] Å² |
|---|---|---|---|---|
| W(1) | 0.05099 (4) | 0.33916 (6) | 0.49547 (4) | 0.0120* |
| W(2) | 0.03869 (5) | 0.27156 (7) | 0.65421 (5) | 0.0172* |
| W(3) | 0.10885 (4) | 0.11972 (6) | 0.47781 (4) | 0.0106* |
| W(4) | 0.10823 (4) | 0.06395 (6) | 0.62963 (4) | 0.0140* |
| W(5) | 0.17467 (5) | 0.21150 (7) | 0.76777 (5) | 0.0184* |
| W(6) | 0.24704 (4) | 0.05914 (6) | 0.59486 (4) | 0.0110* |
| W(7) | 0.32410 (4) | 0.21722 (6) | 0.72594 (4) | 0.0124* |
| P(1) | 0.1776 (3) | 0.2560 (3) | 0.6135 (3) | 0.0062* |
| P(2) | 0.3491 (3) | 0.2074 (4) | 0.5843 (3) | 0.0106* |
| K(1) | 0.0829 (4) | 0.4802 (4) | 0.1329 (3) | 0.0429* |
| K(2) | 0.4117 (3) | 0.1017 (5) | 0.1802 (3) | 0.0400* |
| K(3) | 0.0547 (4) | 0.1909 (5) | 0.1315 (4) | 0.0408* |
| K(4) | 0.1148 (4) | 0.2739 (7) | 0.0007 (5) | 0.0655* |
| K(5) | 0.2542 (7) | 0.067 (1) | 0.4195 (7) | 0.0926* |
| K(6) | 0.419 (1) | 0.4116 (8) | 0.131 (1) | 0.1120* |
| Oa(1) | 0.1488 (7) | 0.3174 (9) | 0.5587 (7) | 0.009 (3) |
| Oa(7) | 0.2484 (7) | 0.273 (1) | 0.6457 (7) | 0.014 (3) |
| Oa(25) | 0.1469 (8) | 0.265 (1) | 0.6664 (8) | 0.020 (4) |
| Oa(346) | 0.1662 (7) | 0.1631 (9) | 0.5874 (7) | 0.009 (3) |
| Ob(12) | 0.0282 (7) | 0.3071 (9) | 0.5674 (7) | 0.013 (3) |
| Ob(13) | 0.0589 (7) | 0.208 (1) | 0.4796 (7) | 0.015 (3) |
| Ob(24) | 0.0502 (8) | 0.147 (1) | 0.6171 (8) | 0.022 (4) |
| Ob(45) | 0.1574 (8) | 0.098 (1) | 0.7084 (8) | 0.019 (4) |
| Ob(57) | 0.2583 (7) | 0.202 (1) | 0.7621 (7) | 0.017 (3) |
| Ob(67) | 0.2854 (7) | 0.107 (1) | 0.6719 (8) | 0.017 (3) |
| Oc(25) | 0.0821 (9) | 0.215 (1) | 0.7343 (9) | 0.028 (4) |
| Oc(34) | 0.0779 (7) | 0.050 (1) | 0.5303 (7) | 0.014 (3) |
| Oc(36) | 0.1901 (7) | 0.062 (1) | 0.5061 (7) | 0.013 (3) |
| Oc(46) | 0.1871 (8) | 0.002 (1) | 0.6197 (8) | 0.018 (3) |
| Od′(1) | 0.0651 (8) | 0.447 (1) | 0.5119 (9) | 0.027 (4) |
| Od′(2) | 0.0466 (9) | 0.373 (1) | 0.6874 (9) | 0.031 (4) |
| Od′(5) | 0.1889 (9) | 0.316 (1) | 0.800 (1) | 0.035 (5) |
| Od′(7) | 0.3490 (9) | 0.320 (1) | 0.7513 (9) | 0.027 (4) |
| Od(1) | −0.0252 (8) | 0.340 (1) | 0.4386 (8) | 0.019 (4) |
| Od(2) | −0.0408 (9) | 0.246 (1) | 0.6443 (9) | 0.030 (4) |
| Od(3) | 0.0714 (8) | 0.075 (1) | 0.4035 (8) | 0.023 (4) |
| Od(4) | 0.0699 (9) | −0.021 (1) | 0.6470 (9) | 0.027 (4) |
| Ow(1) | 0.058 (1) | 0.122 (1) | −0.001 (1) | 0.038 (5) |
| Ow(2) | 0.402 (1) | 0.073 (2) | 0.052 (1) | 0.065 (7) |
| Ow(3) | 0.184 (1) | 0.034 (2) | 0.306 (1) | 0.060 (7) |
| Ow(4) | 0.0000 | 0.066 (2) | 0.2500 | 0.06 (1) |
| Ow(8) | 0.0000 | 0.224 (4) | 0.2500 | 0.11 (2) |
| Ow(5) | 0.178 (1) | 0.178 (1) | 0.111 (1) | 0.048 (6) |
| Ow(6) | 0.299 (2) | 0.033 (2) | 0.275 (2) | 0.10 (1) |
| Ow(7) | 0.297 (2) | 0.208 (3) | 0.057 (2) | 0.15 (2) |
| Ow(9) | 0.180 (2) | 0.401 (2) | 0.099 (2) | 0.09 (1) |
| Ow(10) | 0.303 (3) | 0.379 (4) | 0.034 (3) | 0.16 (2) |
| Ow(11) | 0.031 (2) | 0.443 (3) | 0.316 (2) | 0.11 (1) |
| Ow(12) | 0.5000 | 0.403 (6) | 0.2500 | 0.18 (3) |

[a] Esd's in parentheses refer to the last significant digit. [b] Starred values are for atoms refined anisotropically. They are given in the form of the isotropic equivalent thermal parameter and are derived from the expression $U(eq) = [u_{11}u_{22}u_{33}]^{1/3}$.

The two former values can be compared to those found in another tungstophosphate, the recently described[10] 48-tungsto-8-phosphate, which has also a phosphorus atom linked to two single tungstic octahedra and two groups of edge-sharing octahedra. In this compound, the mean values of the W–Oa lengths are respectively 2.20 and 2.27 Å. In octahedra $W(x)O_6$ ($x$ = 1, 2, 5, 7), the bonds between $W(x)$ tungsten atoms and unshared $Od'(x)$ oxygen atoms are partly multiple, and as for the lacunary $\gamma$-$SiW_{10}O_{36}^{8-}$ anion,[9b] their length mean value, 1.76 Å, is relatively short and is similar to W–Od distances. Trans to these Od′, the $Ob(x,y)$ atoms ($y$ = 3, 4, 6) are at a larger distance from the $W(x)$ (2.15 Å). To the enhancement of the distances $W(x)$–$Ob(x,y)$ corresponds a shortening of the distances $W(y)$–$Ob(x,y)$ (1.79 Å), which are in the range of $W(x)$–$Od'(x)$. Such a trans bond alternation has already been observed[11] and described as a cooperative trans influence. The $PO_4$ junction tetrahedron is quite regular with a

(10) Contant, R.; Tézé, A. *Inorg. Chem.* **1985**, *24*, 4610.
(11) Besecker, C. J.; Day, V. W.; Klemperer, W. G.; Thomson, M. R. *Inorg. Chem.* **1985**, *24*, 44.

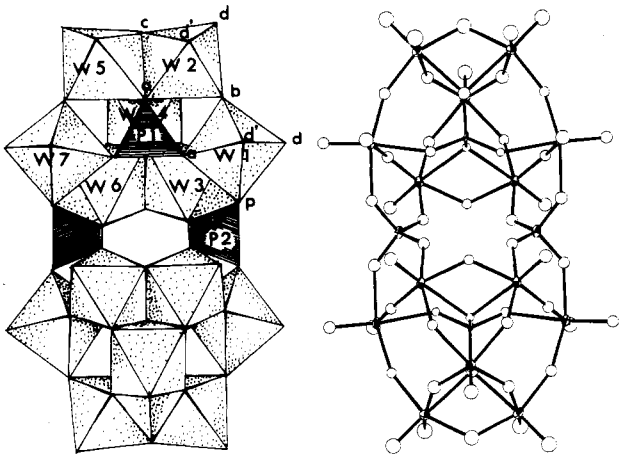


**Figure 1.** Left: Polyhedral model with tungsten and phosphorus numbering and designation of oxygen atoms in the polyanionic structure. Oa and Op oxygens bridge $WO_6$ octahedra and respectively the central P(1) atom and the P(2) atom. Ob and Oc oxygens link $WO_6$ octahedra respectively by vertex and by edge. Od oxygens are bound to one W atom; if two Od oxygens are linked to the same W, the prime is added to the O atom cis to Oa. Right: ORTEP plot of the 14-tungsto-4-phosphate(V) anion with 50% probability ellipsoids for the non-oxygen atoms.

**Table II.** Selected Interatomic Distances (Å)[a] and Average Values of Bond Lengths (Å)[b]

| atoms | dist | atoms | dist | mean value[c] |
|---|---|---|---|---|
| W(1)–Oa(1) | 2.17 (1) | W(7)–Oa(7) | 2.17 (1) | 2.17 |
| W(2)–Oa(25) | 2.32 (2) | W(5)–Oa(25) | 2.26 (2) | 2.29 |
| W(3)–Oa(346) | 2.41 (1) | W(6)–Oa(346) | 2.40 (1) | 2.40 |
| W(4)–Oa(346) | 2.40 (1) | | | |
| W(1)–Ob(12) | 1.88 (1) | W(7)–Ob(57) | 1.89 (2) | 1.90 |
| W(2)–Ob(12) | 1.92 (1) | W(5)–Ob(57) | 1.90 (2) | |
| W(1)–Ob(13) | 2.12 (2) | W(7)–Ob(67) | 2.13 (2) | 2.15 |
| W(2)–Ob(24) | 2.18 (2) | W(5)–Ob(45) | 2.17 (2) | |
| W(3)–Ob(13) | 1.79 (2) | W(6)–Ob(67) | 1.78 (2) | 1.79 |
| W(4)–Ob(24) | 1.79 (2) | W(4)–Ob(45) | 1.79 (2) | |
| W(2)–Oc(25) | 1.91 (2) | W(5)–Oc(25) | 1.93 (2) | 1.93 |
| W(3)–Oc(36) | 1.93 (1) | W(6)–Oc(36) | 1.93 (1) | |
| W(3)–Oc(34) | 1.88 (1) | W(6)–Oc(46) | 1.84 (2) | 1.86 |
| W(4)–Oc(34) | 2.06 (1) | W(4)–Oc(46) | 2.08 (2) | 2.07 |
| W(1)–Od′(1) | 1.74 (2) | W(7)–Od′(7) | 1.76 (2) | 1.76 |
| W(2)–Od′(2) | 1.75 (2) | W(5)–Od′(5) | 1.79 (2) | |
| W(1)–Od(1) | 1.73 (2) | W(7)–Od(7) | 1.75 (2) | 1.72 |
| W(2)–Od(2) | 1.75 (2) | W(5)–Od(5) | 1.71 (2) | |
| W(3)–Od(3) | 1.71 (2) | W(6)–Od(6) | 1.71 (2) | |
| W(4)–Od(4) | 1.70 (2) | | | |
| W(1)–Op(1) | 2.03 (2) | W(7)–Op(7) | 2.04 (2) | 2.04 |
| W(3)–Op(3) | 2.06 (2) | W(6)–Op(6) | 2.04 (2) | |
| P(1)–Oa(1) | 1.51 (1) | P(1)–Oa(7) | 1.51 (2) | 1.53 |
| P(1)–Oa(25) | 1.53 (2) | | | |
| P(1)–Oa(346) | 1.57 (2) | | | |
| P(2)–Op(1) | 1.53 (2) | P(2)–Op(7) | 1.54 (2) | 1.53 |
| P(2)–Op(3) | 1.51 (2) | P(2)–Op(6) | 1.53 (2) | |

[a] Esd's in parentheses refer to the last decimal place. [b] Equivalent bonds in the idealized symmetry are reported on the same line. [c] Average value of bond lengths involving oxygen atoms of the same type.

usual P–O distance (1.53 Å). In the intra unit tetrahedron, although the P(1)–Oa distances are not significantly different (standard deviation 0.02 Å), increasing of the coordination of the Oa atom seems to lengthen the P(1)–Oa bond (from 1.51 Å for the dicoordinated oxygen atom to 1.57 Å for the tetracoordinated one). This geometrical feature, with concomitant lengthening of the W–Oa bond, is related to the weakening of bonds to one atom as its coordination increases. This was already observed in the defect $\gamma$-$SiW_{10}O_{36}^{8-}$.[9b]

**$^{31}$P and $^{183}$W NMR Spectra.** The $^{31}$P NMR spectrum exhibits two lines at $\delta$ = −4.00 and −6.25 with respect to $H_3PO_4$ (Figure 2). The relative integrated intensities, including the satellites for the low-field line, are in the ratio 1/1, in accordance with the

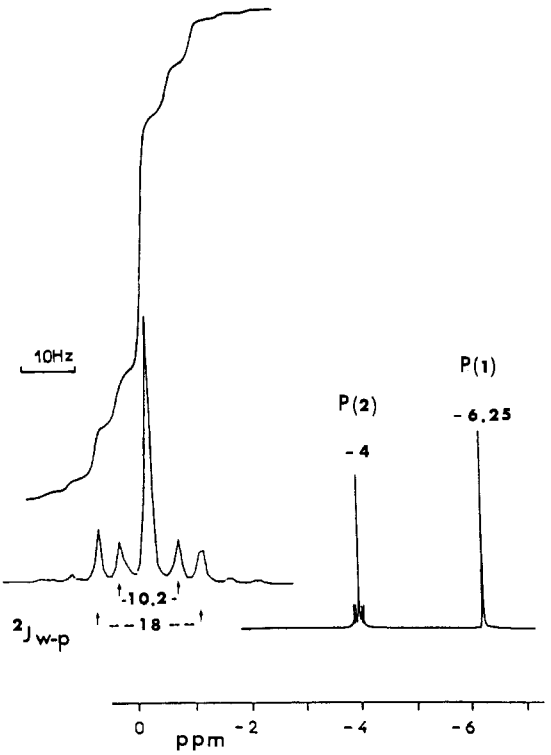


**Figure 2.** 101.2-MHz $^{31}P$ NMR spectrum of a nearly saturated $D_2O$ solution of $P_4W_{14}O_{58}^{12-}$ as the sodium salt with computer expansion of the low-field line showing tungsten satellites (400 scans, without exponential multiplication).

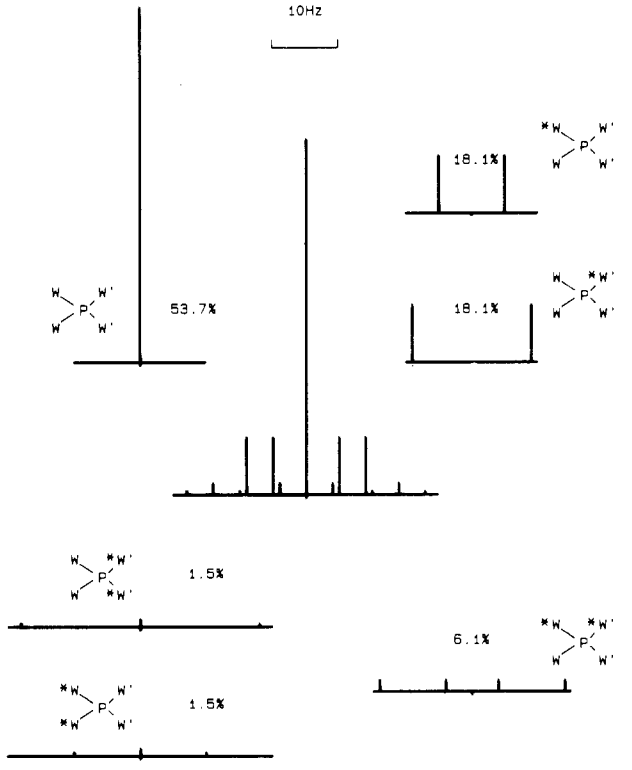


**Figure 3.** Theoretical pattern of the $^{31}P$ resonance for a $P(OW)_2(OW')_2$ fragment, according to the relative abundance of the different isotopomers and with $^2J_{W-P}$ = 10.2 Hz and $^2J_{W'-P}$ = 18 Hz assumed. The $^{183}W$ magnetic nuclei are symbolized by *W. The low-abundance isotopomers with three and four $^{183}W$ atoms are not included.

two kinds of phosphorus atoms in the $P_4W_{14}O_{58}^{12-}$ anion.

The high-field line reveals no fine structure even with resolution enhancement. In contrast, the lower field line is flanked with satellite lines arising from low-abundance isotopomers containing the only magnetically active $^{183}W$ isotope. The central singlet line

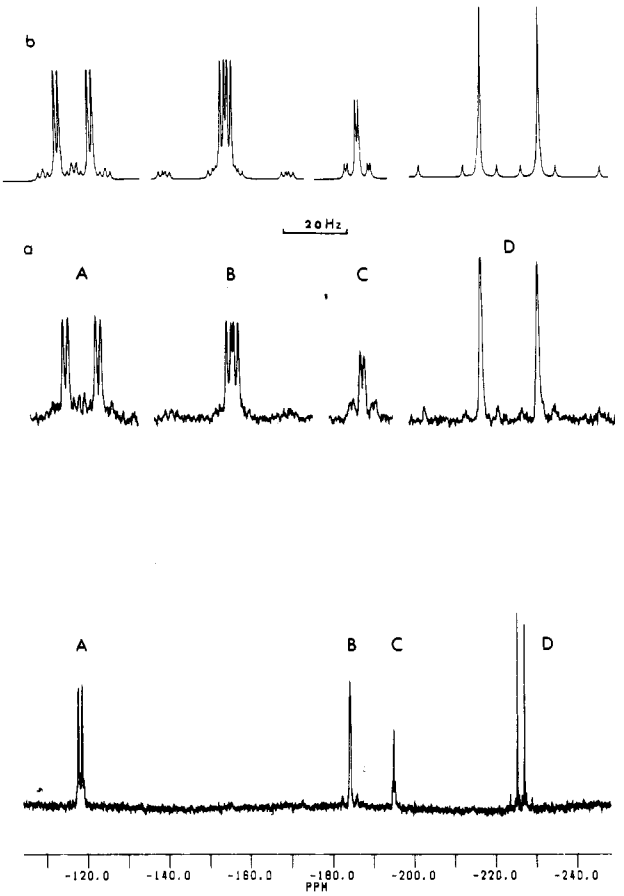


**Figure 4.** (a) 10.4-MHz $^{183}W$ NMR spectra of a nearly saturated $D_2O$ solution of $P_4W_{14}O_{58}^{12-}$ as the sodium salt (27 920 scans, 70° flip angle (70-μs pulse), 8K data points, spectral width 1500 Hz, accumulation time 21 h): lower part, full spectrum (line broadening 0.5 Hz); upper part, computer expansion of each resonance region (24K zero filling, line broadening 0.1 Hz in order to achieve a better line separation, digital resolution 0.09 Hz/Pt). (b) Subspectra simulated by using the parameters of Table IV. A Lorentzian line shape is assumed with 0.5-Hz line width.

comes from isotopomers where the P atom does not "see" any magnetically active W atom.[12] Each pair of doublets, with 10.2- and 18.0-Hz line separations, respectively, centered on the principal signal, arises from a P atom coupled with one $^{183}W$ atom. Moreover, the relative integrated intensities of the satellites and of the central line show that the P atom is linked to two pairs of two equivalent W atoms (Figure 3 and Table III). The $^{183}W$ spectrum (Figure 4) consists of four well-separated absorption regions with intensities in the approximate ratio 2/2/1/2. The determination of tungsten–tungsten coupling constants is frequently impeded by overlapping of lines arising from different components of the same multiplet. From low to high field, there are (i) a doublet of doublets (A) at −118.2 ppm, corresponding to $J_{W-P}$ coupling constant values of 10.2 and 1.6 Hz, with poorly resolved tungsten satellites, (ii) a doublet of doublets (B) at −184.1 ppm ($J_{W-P}$ = 2.2 and 1.5 Hz), with tungsten satellites at ≃7 (shoulder) and 37.2 Hz, (iii) a doublet (C) at −194.9 ppm ($J_{W-P}$ = 1.2 Hz), with tungsten satellites at ≃7 Hz, and (iv) a doublet (D) at −226.1 ppm ($J_{W-P}$ = 18 Hz), with tungsten satellites at 10.3 and 37.0 Hz.

In the crystal structure, the $P_4W_{14}O_{58}^{12-}$ polyanion belongs to the $C_i$ group and the seven tungsten atoms of each $PW_7O_{29}$ subunit

(12) This line is the superposition of many lines with slightly different resonance frequencies, each of them being the resonance of one specific isotopomer, without $^{183}W$ in the vicinity of the phosphorus atom. But these frequency separations due to mass effect (isotopic frequency shift) are probably so small and the number of different isotopomers is so large that the observed effect could be, at the best, a broadening of the line as compared with the natural width. This qualitative remark applies to each line of both spectra.

**Table III.** Relative Occurrence of the Different Isotopomers of a $P(OW)_2(OW')_2$ Fragment

| isotopomer[a] | natural occurrence[b] | $^{31}P$ NMR[c] | isotopomer[a] | natural occurrence[b] | $^{31}P$ NMR[c] |
|---|---|---|---|---|---|
| 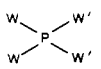 | 53.69 | s | 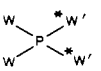 | 1.52 | t |
| 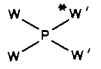 | 18.06 | d | 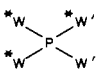 | 0.51 | d of t |
| 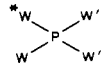 | 18.06 | d | 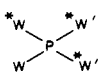 | 0.51 | t of d |
| 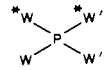 | 6.08 | d of d | 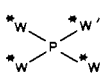 | 0.04 | t of t |
| 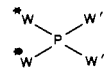 | 1.52 | t | | | |

tot. 99.99

[a] *W stands for the magnetic $^{183}W$ isotope; W, for all nonmagnetic W isotopes, e.g. $^{182}W$, $^{184}W$, and $^{186}W$. [b] Expressed in percent by using the formula $N_{\%}(P(^*W)_x(W)_{2-x}(^*W')_y(W')_{2-y}) = 100(0.144^{x+y})\cdot(0.856^{4-x-y})C_2^xC_2^y$. See: Mc Daniel, D. M. *Inorg. Chem.* **1976**, *15*, 3187. For such calculations the relevant nuclide natural abundances are those expressed in atom percent (14.4 for $^{183}W$) and not in mass percent (14.28 for $^{183}W$). This small relative difference could nevertheless induce relatively large errors for the isotopomer distribution of high-nuclearity entities. [c] s = single line; d = 1/1 doublet; t = 1/2/1 triplet.

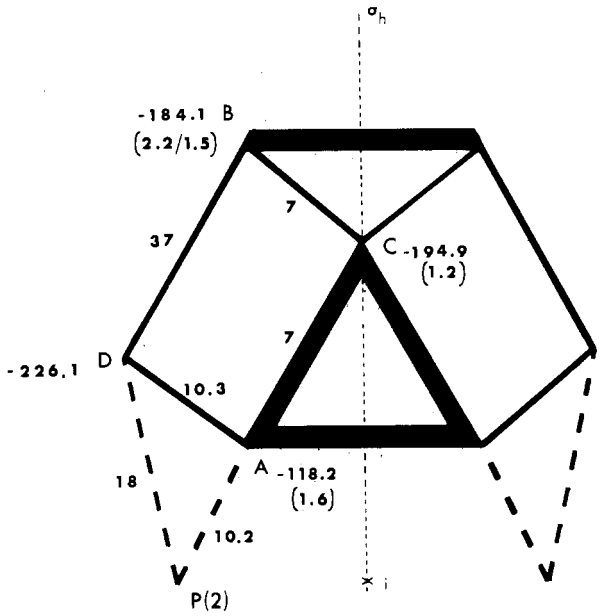


**Figure 5.** Schematic plane representation of the $PW_7O_{29}$ half-anion with the junction P(2) atoms (representation adapted from: Pope, M. T.; Scully, T. F. *Inorg. Chem.* **1975**, *14*, 953). Corner and edge junctions are symbolized by thin and heavy lines, respectively, with the corresponding $^2J_{W-W}$ (or $^2J_{W-P(2)}$) coupling constants (Hz). Near each W atom are given its $^{183}W$ NMR line assignment, chemical shift, and, in parentheses, $J_{W-P}$ coupling constant (Hz).

are independent. The observation of only four resonance lines in the ratio 2/2/1/2 in the solution $^{183}W$ NMR spectrum is only compatible with a preserved dimeric structure in aqueous solution[13] and shows that the polyanion is more symmetrical than in the solid state. Then, the polyanion in solution belongs to the $C_{2h}$ point

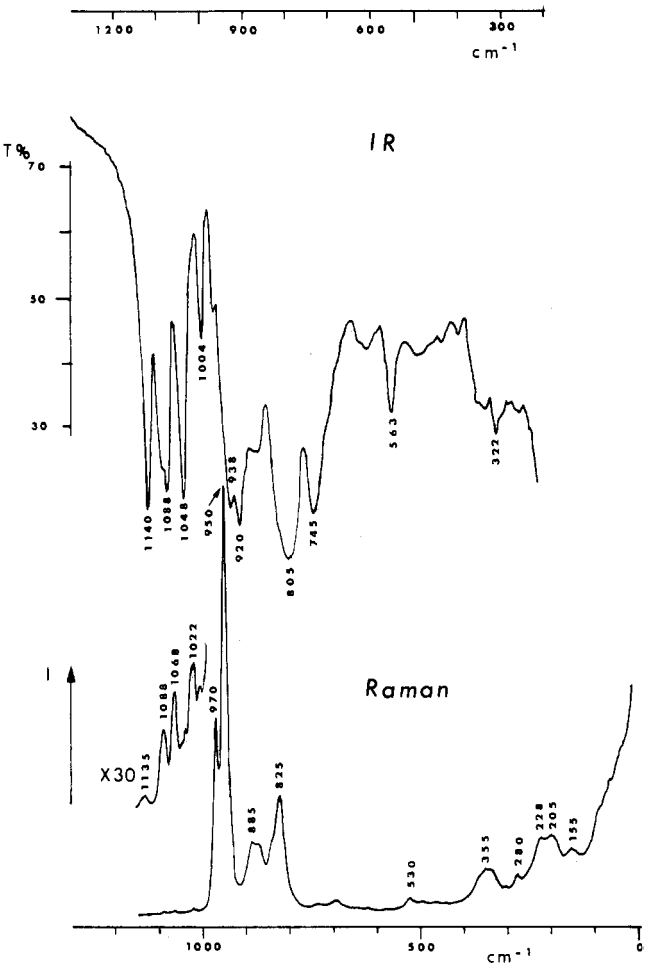


**Figure 6.** Vibrational spectra of the $P_4W_{14}O_{58}^{12-}$ anion: infrared spectrum of the sodium salt (KBr pellet, Perkin-Elmer 283 spectrometer); Raman spectrum of an aqueous solution of the Na salt (Coderg PHO spectrometer, 514.5-nm $Ar^+$ line of a Spectra Physics 164 argon laser).

group, which preserves the crystallographic inversion center; the $\sigma_h$ plane, which contains P(1) and W(4), exchanges W(1) and W(7), W(2) and W(5), and W(3) and W(6), respectively.

The assignment of the two resonance lines in the $^{31}P$ NMR spectrum to the two inequivalent phosphorus atoms P(1) and P(2) can be made on the basis of the observation of a satellite pattern only for the lower field line. The lack of a fine structure is the general case with the already studied polyoxotungstophosphates of the Keggin or the Dawson type, where the phosphorus atom is in a central position, i.e. is surrounded by the tungsten atoms. In fact, the weak W–P coupling ($^2J_{W-P} \lesssim 2$ Hz) cannot be observed in the resonance spectrum of the high-abundance $^{31}P$ nucleus (100%) but can only be observed in the resonance spectrum of the low-abundance $^{183}W$ nucleus (14.4%).[14] The high-field line can be assigned, by analogy, to the central Keggin-like P(1) atom, and then the low field line, to the bridging P(2).

As a starting point for the assignment of the four lines of the $^{183}W$ NMR spectrum, we consider line C of multiplicity 1, which must be attributed to the W(4) atom. Because of the degeneracy of the $^2J_{W-W}$ coupling constants involving line C, we cannot use it to continue the assignment. The solution will be obtained by the help of $^2J_{W-P}$ coupling constants with the hypothesis that the large couplings (10.2 and 18 Hz) are two-bond couplings with P(2). Within this assumption, the extremal resonances A and D are due to the W(3)–W(6) and the W(1)–W(7) atoms or inversely and the remaining resonance B is due to the W(2)–W(5) atoms. The large coupling (37 Hz) observed for both B and D

(13) Actually the $P_4W_{14}O_{58}^{12-}$ is not stable in aqueous solution. New resonance lines appear in the $^{31}P$ NMR spectrum of aged solutions. The evolution is faster in dilute solutions. It is possible that the reaction proceeds through a dimeric ⇔ monomeric fragmentation, which is favored by a low concentration.

(14) (a) Massart, R.; Contant, R.; Fruchart, J. M.; Ciabrini, J. P.; Fournier, M. *Inorg. Chem.* **1977**, *16*, 2916. (b) Acerete, R.; Hammer, C. F.; Baker, L. C. W. *J. Am. Chem. Soc.* **1979**, *101*, 267.

**Table IV.** $^{31}P$ and $^{183}W$ NMR Parameters for $P_4W_{14}O_{58}^{12-}$ [a]

| NMR line | atom | P(2) | P(1) | W(3), W(6) | W(2), W(5) | W(4) | W(1), W(7) |
|---|---|---|---|---|---|---|---|
| P(2) | P(2) | −4.00 | | 10.2 (2W) | | | 18.0 (2W) |
| P(1) | P(1) | | −6.25 | | | | |
| A | W(3), W(6) | 10.2 | 1.6 | −118.2 | | 7.1[b] | 10.3[b] |
| B | W(2), W(5) | 1.5/2.2[c] | 1.5/2.2[c] | | −184.1 | 7.0[b] | 37.2 |
| C | W(4) | | 1.2 | 7 | 7 | −194.9 | |
| D | W(1), W(7) | 18.0 | ... | 10.3 | 37.0 | | −226.1 |

[a] On each line are reported the NMR parameters extracted from the subspectrum of the corresponding nucleus; depending on the partner nucleus, at the beginnings of the columns are reported either the chemical shift (in ppm) or coupling constant (in Hz). [b] Adjusted from a fitting between experimental and simulated subspectra. [c] See text.

resonances can be assigned to the corner junction between the W(2) [≡W(5)] atom and the W(1) [≡W(7)] atom (Figure 1). So, the W(1)–W(7) atoms are responsible for the high-field D resonance and the W(3)–W(6) atoms for the low-field A resonance. This complete assignment allows us to summarize all NMR parameters in Figure 5 and Table IV.

**Vibrational Spectra.** Both IR and Raman spectra (Figure 6) present in the P–O stretching region some bands at relatively high wavenumbers (about 1140 $cm^{-1}$) with respect to the Keggin $PW_{12}O_{40}^{3-}$ anion (1080 $cm^{-1}$) and the free phosphate anion (less than 1020 $cm^{-1}$). Moreover, the stretching modes of the double bond W=Od occur at low wavenumbers by comparison with those for the Keggin anion: respectively 950 and 1010 $cm^{-1}$ for the Raman intense symmetric mode $\nu_s$ (W–O) and 938–920 and 990 $cm^{-1}$ for the IR intense asymmetric one.[15a] These observations agree with the lacunary Keggin structure, for which all stretch vibrators have reduced force constants, with the exception of the P–O vibrators in the vicinity of the lacuna, which are, on the contrary, reinforced.[15b] The wealth and complexity of the P–O stretching region (at least seven distinct modes between 1140 and 970 $cm^{-1}$) agree with the nonequivalence of the two $PO_4$ tetrahedra and the low symmetry of this lacunary heteropolyanion.

## Discussion

The $P_4W_{14}O_{58}^{12-}$ anion consists of two identical $PW_7O_{29}$ subunits, which can be described as fragments of a hypothetical $\beta$-isomer of the $PW_{12}O_{40}^{3-}$ Keggin anion. These very incomplete fragments are not known as free species and are probably stabilized[13] by coordination of phosphorus atoms to tungsten atoms through terminal oxygens. Such a stabilization of Keggin fragments by external heteroatoms has been previously reported for $\beta$-$As_2W_8O_{31}H^{7-}$ [16a] and $NaSb_9W_{21}O_{86}^{18-}$ [16b] polyoxotungstic structures. In the present case, because of their tetrahedral coordination, the phosphorus atoms act as junctions between two subunits, leading to the dimeric stable species.

Assuming that the structural characteristics, bond angles, and bond lengths obtained from the crystal structure determination are, at least approximately, conserved in solution, it is possible to discuss the large variations of the $^2J_{W-W}$ and $^2J_{W-P}$ coupling constants as well as the multiplicity of the B line on the $^{183}W$ NMR spectrum.

Among the four observed tungsten–tungsten couplings, all but one violate the generally accepted empirical rule predicting constants of corner junction coupling in the range 15–30 Hz and edge junction coupling in the range 5–12 Hz.[17] $^2J_{W(3)-W(4)}$ [$\equiv ^2J_{W(4)-W(6)}$] ($\simeq$7 Hz) agrees with an edge junction into a tritungstic group. Of the three corner junction couplings, two are relatively weak ($^2J_{W(1)-W(3)}$ [$\equiv ^2J_{W(6)-W(7)}$] = 10 Hz, $^2J_{W(2)-W(4)}$ [$\equiv ^2J_{W(4)-W(5)}$] = $\simeq$7 Hz) and one is very large ($^2J_{W(1)-W(2)}$ [$\equiv ^2J_{W(5)-W(7)}$] = 37 Hz).

Both low coupling junctions are characterized by one relatively long W–O bond (2.12 Å for W(1)–Ob(13) and W(7)–Ob(67) and 2.18 Å for W(2)–Ob(24) and W(5)–Ob(45)) trans to a terminal oxygen *Od'* and by relatively acute $\mu$-oxo angles (147 and 141°) with respect to those observed in complete Keggin structures.[18] A similar situation has been already described for $\gamma$-decatungstosilicate, for which low corner coupling constants have been correlated with a large W–O distance trans to a terminal oxygen atom.[9b]

On the other hand, the W(1)–Ob(12)–W(2) [≡W(5)–Ob(57)–W(7)] junction presents normal W–O single-bond lengths (ca. 1.90 Å) but a significantly obtuse angle (157°). This geometry, which certainly favors the tungsten–tungsten interaction through $p_\pi$–$d_\pi$ oxygen–tungsten overlap, explains the large value (37 Hz) of $^2J_{W(1)-W(2)}$ [$\equiv ^2J_{W(5)-W(7)}$].

It can be concluded that the classical range of $^2J_{W-W}$ values is a valuable guide for a structural analysis of polytungstates only when no tungsten atom bears more than one terminal oxygen atom. In the other cases, the geometry of some tungsten octahedra becomes very distorted, resulting in modified W–O bond lengths and (or) W–O–W angles, and any low or high tungsten–tungsten coupling constants can be observed.

As for the tungsten–tungsten couplings, the tungsten–phosphorus coupling constants are strongly dependent on the geometry of the $\mu$-oxo bridge. $^2J_{W-P}$ values lower than 2 Hz are observed with central phosphorus atoms in Keggin-like structures and are associated with W–Oa bond lengths in the range 2.2–2.4 Å.[14b] The coupling constants of P(1) with W(3) [≡W(6)] (1.6 Hz) and W(4) (1.2 Hz) have normal values, but the absence of such a coupling for W(1) [≡W(7)] remains unexplained. In the W–O–P(2) junctions, the W–O distances are significantly shorter: 2.03 Å for W(1)–Op(1) [≡W(7)–Op(7)] and W(3)–Op(3) [≡W(6)–Op(6)]. The large $^2J_{W-P(2)}$ coupling constants, 18 and 10.2 Hz, respectively, are clearly associated with these bond lengths.

Finally, let us return to the multiplicity of the B line in the $^{183}W$ NMR spectrum. This doublet of doublets must be attributed to the coupling of W(2) [≡W(5)] with the two phosphorus atoms P(1) and P(2). The first is a two-bond coupling; the second, a four-bond coupling.[19] In the present case, such a long-range spin–spin interaction is probably due to the strong successive two-bond couplings W(2)–W(1) [≡W(5)–W(7)] and W(1)–P(2) [≡W(7)–P(2)] (Figure 5).

As the small $J_{W-P}$ couplings are not observable in the $^{31}P$ NMR spectrum, the question of the assignment of the observed couplings 1.5 and 2.2 Hz to $^2J_{W-P(1)}$ and $^4J_{W-P(2)}$ cannot be answered at this time.

(15) (a) Rocchiccioli-Deltcheff, C.; Thouvenot, R.; Franck, R. *Spectrochim. Acta, Part A* **1976**, *32A*, 587. (b) Rocchiccioli-Deltcheff, C.; Thouvenot, R. *Spectrosc. Lett.* **1979**, *12*, 127.
(16) (a) Leyrie, M.; Tézé, A.; Hervé, G. *Inorg. Chem.* **1985**, *24*, 1275. (b) Fisher, J.; Ricard, L.; Weiss, R. *J. Am. Chem. Soc.* **1976**, *98*, 3050.
(17) (a) Lefebvre, J.; Chauveau, F.; Doppelt, P.; Brevard, C. *J. Am. Chem. Soc.* **1981**, *103*, 4589. (b) Knoth, W. H.; Domaille, P. J.; Roe, D. C. *Inorg. Chem.* **1983**, *22*, 198. (c) Domaille, P. J. *J. Am. Chem. Soc.* **1984**, *106*, 7677.
(18) For Keggin polyoxotungstates, the corner junctions are characterized by W–O ≃ 1.91 Å and W–O–W ≃ 152°. For a review of crystal structures of polyanions, see: Pope, M. T. *Heteropoly and Isopoly Oxometalates*; Springer Verlag: Berlin, 1983.
(19) Four-bond couplings in polyoxotungstates have been scarcely reported: Domaille et al.[20] recently introduced a $^4J_{V-W}$ = 4 Hz into $^{183}W$ line shape calculations to account for the spectra of $HSiW_9V_3O_{40}^{6-}$, and one of us, in 2D-COSY spectra of $\alpha$-$SiW_{11}MoO_{40}^{4-}$ [21a] and $\beta$-$SiW_{12}O_{40}^{4-}$, [21b] observed a correlation between four-bond remote tungsten atoms ($^4J_{W-W}$ = ca. 1 Hz). As underlined by Domaille,[20] nonvanishing four-bond coupling may complicate 2D spectra, and therefore establishing W–W connectivities from such spectra should be performed cautiously, especially in the case of lacunary polyanions.
(20) Finke, R. G.; Rapko, B.; Saxton, R. J., Domaille, P. J. *J. Am. Chem. Soc.* **1986**, *108*, 2947.
(21) (a) Thouvenot, R. *7e séminaire RMN BRUKER*; Bruker: Wissembourg, France, 1984. (b) Thouvenot, R., unpublished results.

## Conclusion

This study establishes the structure of one species obtained from the aqueous solution of tungstate and phosphate mixtures with a low W/P ratio. Several other polyanions coexist in these solutions. We are currently studying some of them, using the same methods of investigation.

**Registry No.** $Na_{12}P_4W_{14}O_{58}$, 111933-31-4; $K_{12}P_4W_{14}O_{58}\cdot 21H_2O$, 111933-32-5; sodium tungstate, 13472-45-2; disodium hydrogen phosphate, 7558-79-4; $^{183}W$, 14265-81-7.

**Supplementary Material Available:** A table of anisotropic temperature factors for W, P, and K atoms (1 page); a listing of structure factor amplitudes (16 pages). Ordering information is given on any current masthead page.

Contribution from the Department of General and Inorganic Chemistry, Faculty of Chemistry, University of Thessaloniki, P.O. Box 135, 54006 Thessaloniki, Greece, Applied Physics Laboratory, Department of Physics, University of Thessaloniki, 54006 Thessaloniki, Greece, and Institute of Chemistry, University of Wroclaw, 14 F. Joliot-Curie Street, 50383 Wroclaw, Poland

# Crystal Structure, Magnetic Properties, and Orbital Interactions of the [(μ-Terephthalato)(ethylenediamine)diaquocopper(II)] Zigzag Chain

Evangelos G. Bakalbassis,[1a] Anastasios P. Bozopoulos,[1b] Jerzy Mrozinski,[1c] Panayotis J. Rentzeperis,[1b] and Constantinos A. Tsipis*[1a]

*Received June 25, 1987*

The crystal structure of $[Cu(en)(H_2O)_2(TA)]_n$, where $TA^{2-}$ is the dianion of terephthalic acid and en is ethylenediamine, has been determined by direct X-ray methods. The complex crystallizes in the monoclinic space group $P2/c$ with two formula units in a unit cell of dimensions $a$ = 5.726 (1) Å, $b$ = 8.806 (2) Å, $c$ = 12.866 (4) Å, and $\beta$ = 101.12 (1)° and densities $d$(calcd) = 1.693 × $10^3$ kg·m$^{-3}$ and $d$(exptl) = 1.694 × $10^3$ kg·m$^{-3}$. The structure was refined to conventional discrepancy factors of $R$ = 0.041 and $R_w$ = 0.049 for 1404 observed reflections. A crystallographic inversion center is located at the center of the benzene ring of the TA bridging ligand. The Cu centers, lying on 2-fold axes, are bridged by TA in a bis-unidentate fashion. Thus, infinite zigzag chains along the $b$ axis and parallel to ($\bar{1}02$) are formed. The environment of each metal ion is distorted-elongated octahedral. Variable-temperature (4.2–295 K) magnetic susceptibility data are consistent with a chain structure, the intrachain exchange parameter $J$ being 4.0 cm$^{-1}$ and the interchain exchange parameter $zJ'$ being −7.0 cm$^{-1}$. The EPR spectrum does not exhibit any evidence for a triplet state. An orbital interpretation of the coupling is proposed.

## Introduction

In recent studies[2,3] our attention has been focused on the investigation of the magnetic exchange mechanism of novel terephthalato-bridged $d^9$–$d^9$ magnetic systems. Within this framework important magnetostructural relationships have been deduced on the grounds of experimental and quantum-chemical methods. It was shown that, under certain conditions, the terephthalato dianion is an appropriate bridging unit to design magnetic systems with expected magnetic properties. These magnetic systems could be either dimeric or polymeric, depending on the reaction conditions. In the polymeric magnetic systems some specific problems exist; in only rare cases can single crystals be obtained, and therefore uncertainties in the determination of the exchange parameters of the systems are unavoidable. In our opinion these are the main reasons justifying the absence from the literature of the magnetic properties of the copper(II) μ-terephthalato chains.

In this work we report the synthesis, crystal structure, and magnetic properties of the polymeric [(μ-terephthalato)(ethylenediamine)diaquocopper(II)] complex. Moreover, a possible interpretation of its magnetic behavior in correlation with the structural data and extended Hückel LCAO–MO calculations was attempted.

## Experimental Section

**Synthesis.** The compound was prepared as follows. A 4 × $10^{-3}$ mol sample of $Cu(NO_3)_2\cdot 3H_2O$ was added to an equimolar one of ethylenediamine in 10 mL of distilled water and 40 mL of ethanol. The dark blue, clear solution derived was added to a 2 × $10^{-3}$ mol sample of disodium terephthalate in 10 mL of distilled water and 100 mL of ethanol (under continuous stirring at room temperature). The complete mixture was refluxed for 7 h. The light blue powder precipitate formed was filtered off; the dark blue filtrate, upon staying in a refrigerator for a period of about 1 month, gave 0.2 g (31% yield) of dark blue single crystals suitable for structure and magnetic determinations. Anal. Calcd for $C_{10}H_{16}N_2O_6Cu$: C, 37.10; H, 4.98; N, 8.65; O, 29.65; Cu, 19.62. Found: C, 37.02; H, 5.09; N, 8.53; O, 29.95; Cu, 19.41.

**Table I.** Crystallographic Data Collection

| | |
|---|---|
| formula | $[Cu(C_8H_4O_4)(C_4H_8N_2)(H_2O)_2]_n$ |
| cryst color | dark blue |
| cryst habit | prismatic |
| cryst size, mm | 0.60 × 0.25 × 0.20 |
| $d_{exptl}$, kg·m$^{-3}$ | 1.694 × $10^3$ |
| $\mu$(Mo Kα), cm$^{-1}$ | 18.2 |
| cryst syst | monoclinic |
| space group | $P2/c$ |
| $a$, Å | 5.726 (1) |
| $b$, Å | 8.806 (2) |
| $c$, Å | 12.866 (4) |
| $\beta$, deg | 101.12 (1) |
| $V$, Å$^3$ | 636.58 |
| $Z$ | 2 |
| diffractometer | Philips PW1100 |
| monochromator | graphite |
| radiation (λ, Å) | Mo Kα (0.710 70) |
| temp, °C | 21 |
| scan type | $\theta$–$2\theta$ |
| $2\theta$ range, deg | 6–60 |
| scan speed, deg·s$^{-1}$ | 0.03 |
| bkgd | half of scan time, in two parts, before and after every scan, in fixed position |
| no. of std. reflcns | 3, measd every 2 h |
| reflcns measd, $+h$, $\pm k$, $\pm l$ | 0→8,12,15 |
| no. of reflcns collcd | 3940 |
| no. of indep reflcns merged | 1799 |
| $R_i$ | 6.1 (2924 reflcns) |
| no. of reflcns kept for refinement | 1404 [$I > 3\sigma(I)$] |

(1) (a) Department of General and Inorganic Chemistry, University of Thessaloniki. (b) Department of Physics, University of Thessaloniki. (c) University of Wroclaw.
(2) Bakalbassis, E. G.; Mrozinski, J.; Tsipis, C. A. *Inorg. Chem.* **1985**, *24*, 4231.
(3) Bakalbassis, E. G.; Mrozinski, J.; Tsipis, C. A. *Inorg. Chem.* **1986**, *25*, 3684.

0020-1669/88/1327-0529$01.50/0 